Geometry and mechanics of the active fault system in western Slovenia

Blaž Vičič,[1,2] Abdelkrim Aoudia,[2] Farhan Javed,[2,3] Mohammad Foroutan[2,*] and Giovanni Costa[1]

[1] *Department of Mathematics and Geosciences, University of Trieste, I-34128 Trieste, Italy. E-mail: bvicic@ictp.it*
[2] *The Abdus Salam International Centre for Theoretical Physics, I-34151 Trieste, Italy*
[3] *Centre for Earthquake Studies, National Centre for Physics, Islamabad, Pakistan*

Accepted 2019 March 2

SUMMARY

Western Slovenia is part of an actively deforming region accommodating anticlockwise rotation of Adria and its continuous collision with Eurasia. The geometry of the active faulting system in this plate boundary is not well defined. In this study, detailed analysis of earthquake activity was performed with relocation of earthquakes in the period between 2006 and 2017. With inspection of the waveform data, slight temporal clustering of activity was observed. To increase the detection rate of microearthquakes we used a matched filter detection algorithm method. Templates of earthquakes were created and a database of continuous waveform data within the period 2006–2017 was investigated. As a result, high temporal correlation allowed us to identify swarms and earthquake sequences that affected the active fault system in the study region.

Relocated seismicity allowed us to constrain the geometry of 5 nearly parallel faults, namely: Ravne, Idrija, Predjama, Selce and Raša faults. All these faults do have an expression in the geomorphology and reach a seismogenic depth of up to 20 km. Vertical and along strike extents of these active faults can favour earthquakes of moment magnitude equal to 7 or larger. The most recent large earthquake that occurred in this region is the 1511 earthquake with a magnitude 6.8.

The leading fault in the system being the Idrija right-lateral strike-slip fault, experiences earthquake activity from 5 to 20 km on its northern segment, while on its southern segment no earthquake activity is detected over the decade of observations. We show that the interseismic loading on the southern segment of Idrija fault is likely unclamping the locked adjacent faults promoting the observed bursts of seismicity. Moreover, in 2009 the Predjama fault accommodated a sudden increase of the surface deformation at the extensometer accompanied by a simultaneous swarm activity at its seismogenic depth. This behaviour might correspond to velocity strengthening and weakening processes taking place at both the surface and depth terminations of a locked vertical fault. These processes can be driven by a slow-slip event on the deeper part of Idrija fault that would generate a temporary acceleration of the interseismic loading rate along with a change within the fluid circulation.

Key words: Europe; Earthquake hazards; Seismicity and tectonics.

INTRODUCTION

Western Slovenia is part of the north-eastern Adriatic region and includes the External Dinaric domain and part of its junction with the Southeastern Alps. Active deformation is accommodated by right-lateral strike-slip and thrust faulting as a response to the anticlockwise rotation of Adria and its continuous collision with Eurasia at rates of 2–4 mm yr^{-1} (Vrabec & Fodor 2006; Weber *et al.* 2010; Metois *et al.* 2015). The regional geomorphology is controlled by the Idrija right-lateral fault striking NW–SE crossing most of western Slovenia and other parallel faults such as Ravne, Predjama and Raša faults from NE to SW (Bajc *et al.* 2001; Fitzko *et al.* 2005; Vrabec *et al.* 2006; Moulin *et al.* 2014, 2016). These faults

* Now at School of Geology, College of Science, University of Tehran, PO Box 14155-6455, Tehran, Iran

transfer around 3.8 mm yr^{-1} right-lateral displacement as derived from geomorphological markers (Moulin *et al.* 2014, 2016).

Western Slovenia was struck by destructive local and regional earthquakes (Fig. 1a) that caused casualties and damage to the infrastructure and environment. The strongest local earthquake with M_w 6.8 that ruptured a segment of Idrija fault, happened in 1511 with an epicentral location around the town of Idrija, in the central part of western Slovenia (Ribarič 1982; Fitzko *et al.* 2005; Bavec *et al.* 2013). In 1976, the region was affected by the nearby Friuli thrust faulting earthquake sequence in northeastern Italy that consisted of a magnitude 6.5 main shock followed by 2 large magnitude 6.1 aftershocks (Aoudia *et al.* 2000; Basili *et al.* 2008). Last destructive earthquakes happened in 1998 with M_w 5.6 main shock and a M_w 5.2 in 2004 in the region of Bovec along the Ravne right-lateral strike-slip fault (Bajc *et al.* 2001; Zupančič et al 2001; Kastelic *et al.* 2004) in the northern part of western Slovenia. In the southern part of the same region 2 historical earthquakes with magnitude >5 are reported in the literature (Ribarič 1982). Both the location and the mechanism of these events are unknown.

Modernization of the seismic network in western Slovenia stared after the 1998 earthquake. It reached today's extent in 2006 with several stations recording in real time. Since then multiple small magnitude main shock–aftershock sequences took place in the region, mostly in its northern and southern part with rare 'similar sized' earthquake sequences (e.g. Jesenko *et al.* 2006, 2010) happening in the central and southern part, as reported by 'Agencija Republike Slovenije za okolje' (ARSO).

In this paper, we performed a detailed analysis of the data sets recorded by different seismic networks (namely we used data from three Italian networks managed by University of Trieste, Civil protection of Friuli Venezia Giulia and 'Instituto Nazionale di Oceanografia e di Geofisica Sperimentale' (OGS) as well as data by ARSO surrounding the faulting system in western Slovenia. We analysed the data using fully automated short-time average to long-time average (STA/LTA) detection algorithm, followed by visual inspection of the data to detect missed events, and lastly a matched filter detection algorithm for the detection of even smallest earthquakes, which resemble the selected templates. All the detected earthquakes were precisely relocated, using a recent regional 3-D velocity model (Guidarelli *et al.* 2017).

Newly detected and relocated earthquakes (Fig. 1b) allowed us to study background earthquake activity as well as newly observed swarm sequences that took place in western Slovenia from 2006 up to the end of 2017. We propose a new model of active faults in western Slovenia on the base of the relocated seismicity and surface geology and geomorphology. We explore the short-term behaviour of these faults using Coulomb stress modelling that we compare to the observed clustering in time and space of the earthquake activity in the region.

EARTHQUAKE DETECTION AND RELOCATION

To detect microearthquakes, the matched filter detection algorithm was used (Shelly *et al.* 2007; Chamberlain *et al.* 2017). To create the templates, we first scanned the continuous waveform data (2006–2017) with the standard energy-based STA/LTA detector, tweaked for detection of local earthquakes (prefiltered between 2.0 and 20.0 Hz, with short-time window set at 0.3 s and long-time window at 10.0 s with amplitude threshold set at 6). Successful detections were manually re-picked and used in the creation of templates. Additionally, the continuous waveform dataset was manually inspected to find events that were not automatically detected and missed in previous STA/LTA run. For events, for which at least 4 picks were possible, location and magnitude were calculated by Antelope® software package (BRTT Antelope software 1995) using IASP91 velocity model (Kennet 1991). The location of earthquakes was then recalculated using NonLinLoc software package (Lomax 2004) and hypoDD (Version 2.1b, Waldhauser 2001). For relocation, we used a newly computed regional 3-D velocity model (Guidarelli *et al.* 2017) obtained from ambient noise tomography.

For matched filter detection, all events with $M_L > 0.8$ were selected, leaving us with 672 template earthquakes distributed along western Slovenia, for all the sequences and background earthquake activity. Since all the continuous waveforms were processed in advance, lower number of broadband stations was used for matched filter detection. This still allowed us to use obtained detections for relocation of the events using *P* and *S* arrival times computed from cross correlating the detection times with templates. Prior to running the matched filter detection algorithm, waveforms were pre-processed. Both templates and continuous waveforms were downsampled from 200 or 100 Hz to 20 Hz and bandpass filtered between 2.0 and 8.0 Hz. All the local earthquakes in the region are high-frequency earthquakes, but bandpass filtering lowers the computational cost, gives more coherent and higher number of detections, but still provides us with the ability to distinguish between individual families of earthquakes. Waveforms with length less than 19 hr of the 24 hr were discarded to not introduce artefacts in the detections. Length of templates was 2.5 s with 0.1 s pre-pick times. *P* arrival times templates were extracted from the vertical component while *S* arrival time templates were extracted from the horizontal component. With the templates all the years between 2006 and 2017 were processed.

In search for previously missed earthquakes using a matched filter algorithm, we used EQcorrscan software package (version 0.2.7) (Chamberlain *et al.* 2017). In the calculations of cross correlation, all the channels of the templates are correlated with day-long continuous waveforms on the same stations and channels. For successful detection, normalized cross-correlation values for each day are summed on all the channels, which gives us a network cross-correlation time-series. When the network cross-correlation sum exceeds pre-set 9 x median Absolute Deviation (MAD) a detection is declared. The 9 x MAD value also introduces detections that are not real events, but these events were later removed by visual inspection of computed raw spectrograms.

Simultaneous to matched filter detection also *P* and *S* arrival times were obtained for newly detected events by cross correlating the template with the detection which gave us more precise picks. We used 0.2 s before and 1.0 s after the picked time to get new arrival at the maximum of cross correlation value. For new *P* and *S* arrival times only events with value above 0.7 of similarity were used. New *P* and *S* arrival times were then used as an input to HypoDD to calculate locations of the events using absolute traveltimes. Magnitudes were estimated using the local magnitude by calculating logarithm of maximum amplitude recorded on either vertical or horizontal component and applying the epicentral distance correction ($M_L = \log_{10}(A) + \text{corr}$) (Di Bona 2016).

Finally, by using STA/LTA automatic detection we detected 6125 events (including quarry blasts). Manual inspection of the waveforms added 1800 events. After the matched filter processing, our catalogue consists of approximately 10 000 detected events.

Due to the majority of earthquakes being too small to be clearly observed on all the stations that the template was extracted from, we can define the detections as near repeating earthquakes happening in

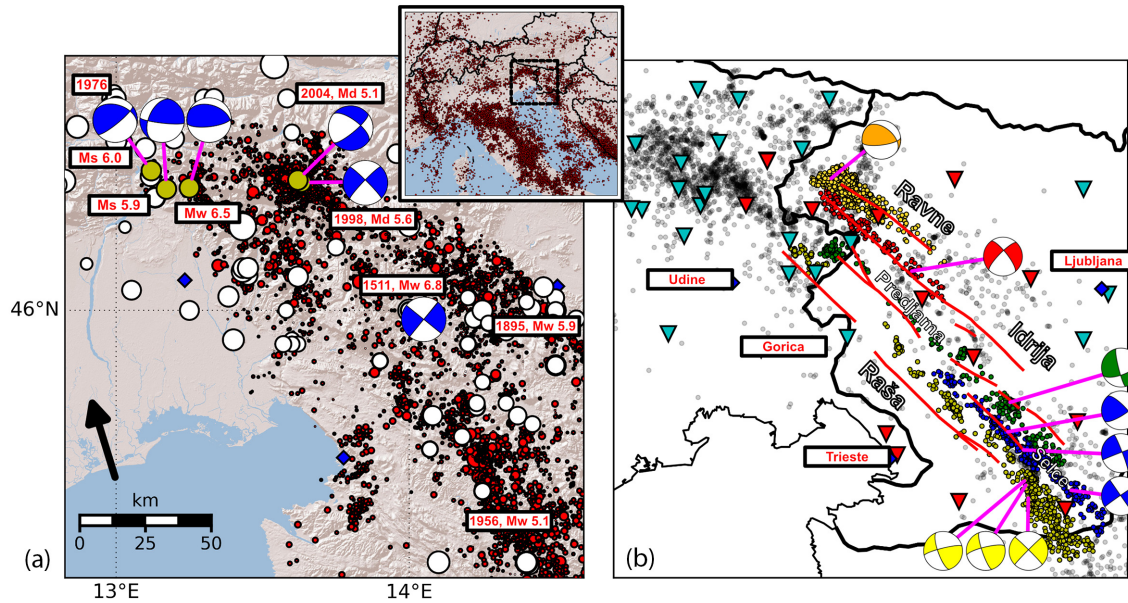

Figure 1. Panel (a) shows historical earthquake activity in a broader region around western Slovenia and NE Italy. In white, SHEEC catalogue (Stucchi *et al.* 2013) of earthquakes with $M > 4$ are shown while focal solutions represents the modelled solutions of major earthquakes, namely Idrija, Friuli and Bovec earthquakes. In red, seismic events as reported by ARSO are shown. Black arrow represents a GPS velocity field (Metois *et al.* 2015). Fig. 1b shows all the detected and relocated earthquakes colour-coded regarding the causative fault. In orange, earthquakes of Ravne fault are shown, in red Idrija fault (northern segment), green Predjama fault, blue Selce fault and yellow Raša fault. Black events are relocated background seismicity or earthquakes contributed to other fault systems. Triangles are stations used in the study—cyan stations were only used for STA/LTA detection and manual inspection of earthquake activity while red stations were used also for matched-filter earthquake detection.

near vicinity of the original template (cross-correlation value above 70 per cent). In the northern part, tiny near-repeating earthquakes are happening on both, Idrija and Ravne fault. Repeatability of events on Ravne fault is much higher than on Idrija fault due to the larger number of templates and higher seismicity rate than on Idrija fault. These near repeating events could all be aftershock of 1998–2004 sequence since the continuous data starts with 2006 or may be present even before the 1998–2004 sequence, but their detection would not be possible due to non-existing near fault seismic stations. One cluster of near repeating events through all the studied years was recognized in the northernmost part of the Ravne fault. On the same fault, another cluster of near-repeaters was observed, but their number is much smaller and not distributed through all the years. In the southern part of the area, only rare near-repeaters were found but a big increase in the number of aftershocks of different main shocks was observed, some lasting for years.

The detection and relocation procedure has revealed that further to the background earthquake activity and small main shock–aftershock sequences also a swarm-like sequences are present in the study region. Swarms and swarm-like sequences are recognized only in the central and southern part of the studied area, along Raša, Selce and Predjama faults. They happened in 2006 as Vipava swarm on Raša fault, in 2010 as Postojna swarm along Predjama fault and in 2017 as Selce swarm along Selce fault and in the southmost extend of the area, probably along Raša fault as Ilirska Bistrica swarm and Rijeka swarm (unknown fault). Details are provided in the next section.

SWARMS

As already mentioned, we discovered swarms and swarm-like seismic sequences (Fig. 2) happening along the different faults in western Slovenia (Fig. S8). Swarms last from days to years and are in general lower magnitude than the main shock–aftershock sequences that happened between 2006 and 2017 in the region. The depth of swarms ranges between 8 and 16 km, similar to the main shock–aftershock sequences.

Vipava swarm

Vipava swarm (Fig. 2a) started at the beginning of September 2006 and lasted for 2.5 months consisting of 622 detected earthquakes, with magnitudes ranging between M_L –1.0 and 1.7, with few earthquakes exceeding M_L 1.0. No focal solutions exist for this swarm because of its low magnitudes and distances from the recording stations. Depth distribution was between 8 and 13 km and its projection to the surface coincides with the Raša fault.

Postojna swarm

Postojna swarm-like sequence (Fig. 2b) starting at the end of 2009 and finishing at the beginning of 2011 was the longest sequence in western Slovenia between 2006 and 2017, with more than 3000 detected earthquakes beneath the town Postojna, along the Predjama fault. The swarm started on 14th of July 2009 with few small earthquakes with maximum M_L 1.0. The peak of activity was on 15th of January 2010 when main shock with M_L 3.5 and strike slip focal mechanism with dip component, happened. 15 earthquakes with $M_L > 1.0$ happened during the swarm, with 14 of them happening in first 3 months of the year. Last $M_L > 1.0$ earthquake happened on 3rd of November 2010. Activity stopped with the ending of 2010 with 2 small events happening in June 2011. After that there were no earthquakes in the area where the 2010 swarm took place. Excluding the main shock of the series, magnitudes of bigger earthquakes

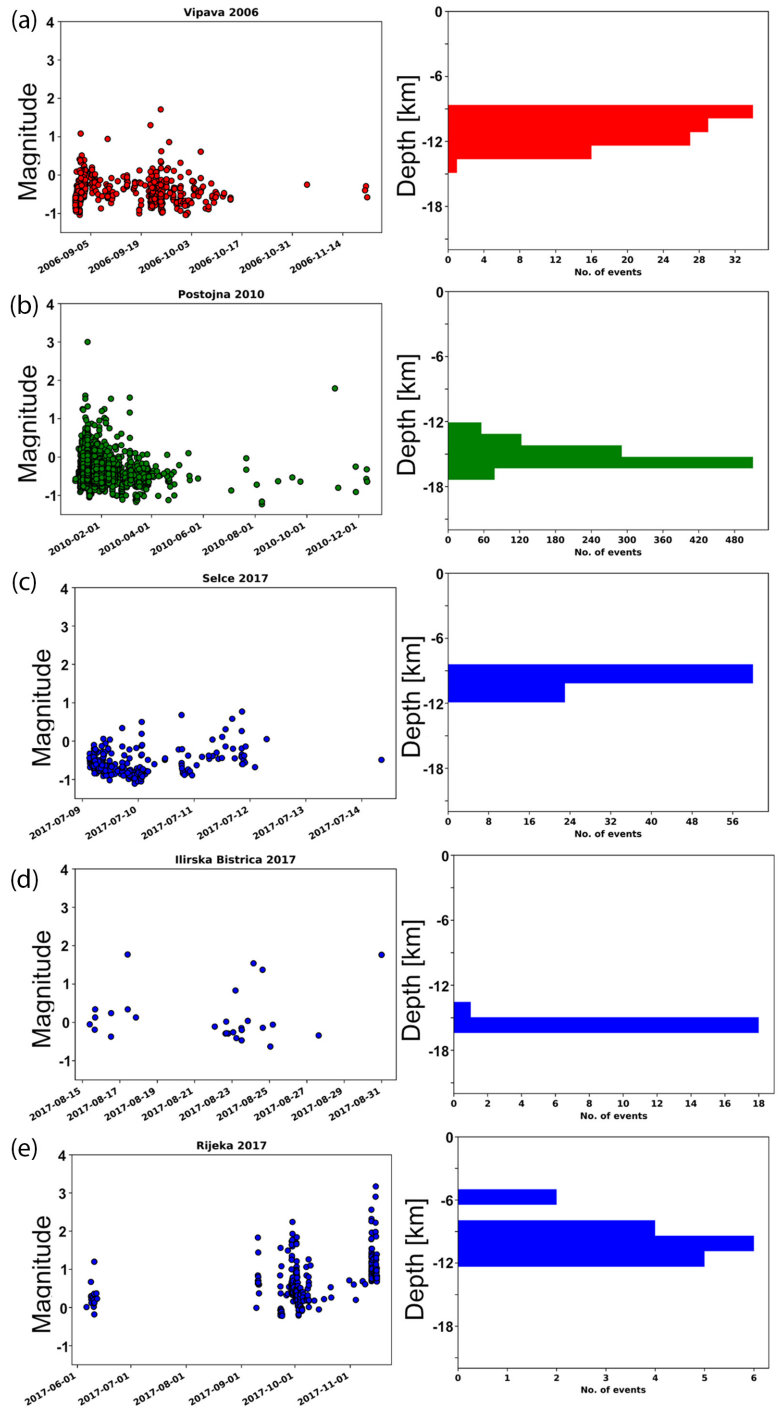

Figure 2. Magnitude versus time and depth distribution for different swarms: Vipava swarm (a) located on Raša fault took place in 2006 and lasted for 3 months. Strongest earthquake reached M_L 1.7 with depth distribution between 9 and 14 km. Postojna swarm 2009–2011 (b) was the longest swarm in the region, with earthquake activity lasting for more than a year. Strongest recorded earthquake had a M_w 3.5 and strike-slip with dip component focal mechanism. The depth distribution peaks at 15 km. In 2017 multiple swarms happened in southern part of the fault system along Selce (c), Raša fault (d) and unknown fault (e). Selce and Ilirska Bistrica swarms were low magnitude and short in time events, while Rijeka swarm lasted for half a year with magnitudes reaching M_L 3.

are between M_L 1.0 and M_L 2.0 and are constant throughout first 3 months of the swarm. Depth of the activity was at around 15 km.

Selce swarm

Until summer 2017 there were no swarms or swarm-like sequences in the studied area (main shock–aftershock sequences and background activity is present through the years). The activity started on July 9th (Fig. 2c) and its projection to the surface coincides with the Selce fault. The swarm lasted for only 6 d with 274 detected

earthquakes with M_L between –1.0 and 0.8 with 14 earthquakes with M_L above 0.0. Depth of earthquakes was at around 10 km.

Ilirska Bistrica swarm

A month after the Selce swarm, another small sized swarm took place south of Selce swarm, along the Raša fault in southernmost part of western Slovenia. Swarm lasted from 15th August until 31st August 2017 (Fig. 2d). The number of the events was much lower compared with other swarms, with only 28 earthquakes with M_L between –0.6 and 1.77, with 12 of the earthquakes above M_L 0.0. The depth distribution of the events was at around 15 km.

Rijeka swarm

The last of the detected swarms started in June 2017 (Fig. 2e) far in the south of the studied area, close to the town of Rijeka in Croatia. It lasted for 6 months with M_L between –0.22 and 3.2 (the threshold of detection in this area is lower, due to the unavailability of data) with 412 detected events and 82 above M_L 1.0. It is worth noting that the same area (town of Rijeka) was later struck by 3 $M_L > 4.0$ earthquakes, just some 15 km to the south of the swarm. The three stronger earthquakes happened in mid-August 2017, during the quiescent period of the Rijeka swarm.

GEOMETRY AND MECHANICS OF THE FAULT SYSTEM

Geometry of the fault system

From its geologic and geomorphic signature (Placer *et al.* 2010; Moulin *et al.* 2016) the active fault system in western Slovenia consists of four important parallel faults, namely Idrija, Ravne, Predjama and Raša faults. Idrija fault is interpreted as a nearly vertical fault striking NW–SE and sampling the whole crust as recently reported from ambient noise tomography (Guidarelli *et al.* 2017). Ravne fault is located to the northeast of Idrija fault while the remaining faults stand on the southern part and are interpreted as structures that flatten at a mid-crustal depth and connect to Idrija (Moulin *et al.* 2016) or as independent parallel and nearly vertical structures (Placer *et al.* 2010).

With the newly detected and relocated microearthquakes we are able to image and constrain the geometry of the known active faults at the surface and identify a new active fault in between Raša and Predjama faults.

To the northwest of the faulting system (Fig. 3a) the relocated seismicity exhibits three clusters on a SW–NE section: One on the continuation of the Raša fault to the NW, the second is most probably associated with the Predjama fault and the third cluster samples Idrija fault with events reaching 20 km depth. The Idrija cluster gets distributed and shuts down at shallower depths (10 km) beneath the Ravne to the NE without constraining a clear faulting geometry. This pattern of seismicity, from localized to distributed, may be explained by the vicinity of the Ravne fault to the junction between NW–SE Dinaric structures to E–W Alpine structures as reported in geology (Placer *et al.* 2010), in geodesy (Borghi *et al.* 2009) and in seismology (from focal solutions of recent $M_w > 3.0$ earthquakes reported by Sarao & Staff 2013; Sarao (2016)).

Fig. 3 highlights that Idrija fault has two distinct behaviours within the decade of observations: the northern segment characterized by well-localized seismicity along its strike and a southern segment without earthquake activity. A clear change within the strike of Idrija fault with a sizeable stepover as mapped by geology (Mlakar *et al.* 2009) and also reported in geomorphology (Moulin *et al.* 2014) separates the two segments. This structural complexity is located in the surroundings of the city of Idrija where the fault name comes from.

Unlike the northern segment of the Idrija fault, Predjama fault exhibits a slightly more diffusive seismicity probably due to the higher segmentation and complexity of the fault itself (Figs 3a and b). The majority of earthquakes happened between 12 and 20 km depth and are distributed along all its length.

Earthquakes connected to Selce fault (Šebela 2016), with surface expression visible in the central and southern part, are happening between 8 and 20 km depth (Fig. 3b), depending on the sequence. It seems that stronger earthquakes (2008 M_L 3.0 and 2014 M_L 4.7) nucleate deeper, while smaller magnitude sequences are shallower.

The Raša fault exhibits a clear geomorphic signature in the central part of the study area. Like Selce fault, earthquake activity is distributed between 4 and 18 km depth (Fig. 3b). Earthquakes connected to the Raša fault are illuminating a fault going from sub vertical in the shallow part towards a northeast dipping fault at depth (Fig. 3b) in the central part of the system. A connection with Selce fault is observed at depth.

In the southern part of the fault system, earthquake activity is distributed at the surface (Figs 3c and d). Specifically, the seismicity is represented by three subclusters located at 5, 10 and 15 km depth that took place over 1 month time span with a clear migration from NE to SW and from deeper to shallower depths (15 to 5 km). The 15 km sequence follows two main shocks of equal M_L 3.5. The 10 km sequence follows a M_L 2.7 main shock. The 5 km sequence follows a M_L 1.5 magnitude main shock. These three sequences are imaging what we interpret as southwest dipping antithetic faults to the Raša main fault (Fig. 3c). It is not clear if this migration is caused by pore pressure diffusion (Rutledge *et al.* 2004), aseismic slip propagation (Lohman & McGuire 2007; Yoshida *et al.* 2018) or just a response to the fault unclamping, as is described in the later chapter.

We propose a series of near parallel strike slip faults as a geometry of active faults of western Slovenia (Fig. 4). Our model is based on the geological and geomorphological interpretations of Idrija being the leading fault of the system, which also agrees with the interpretations of the crustal and upper mantle studies using ambient noise tomography. Using a number of well-located earthquakes we can observe that Raša, Selce and Predjama fault show similar strike to the Idrija fault with Raša fault dipping towards NE and connecting to the vertical Selce fault at the depth of 20 km. Similarly to Selce fault, also Predjama fault is a vertical structure but without connection to other faults. Our model agrees with the geological interpretation (Placer *et al*. 2010) where the Predjama and Raša faults are vertical structures, but the precisely relocated earthquakes show, that Raša fault changes its dip from vertical to NE dipping plane.

Transient

From 2006 to end of 2017 we observe that the area of western Slovenia is experiencing long-lasting periods of background seismicity with rare main shock–aftershock sequences and shorter transient

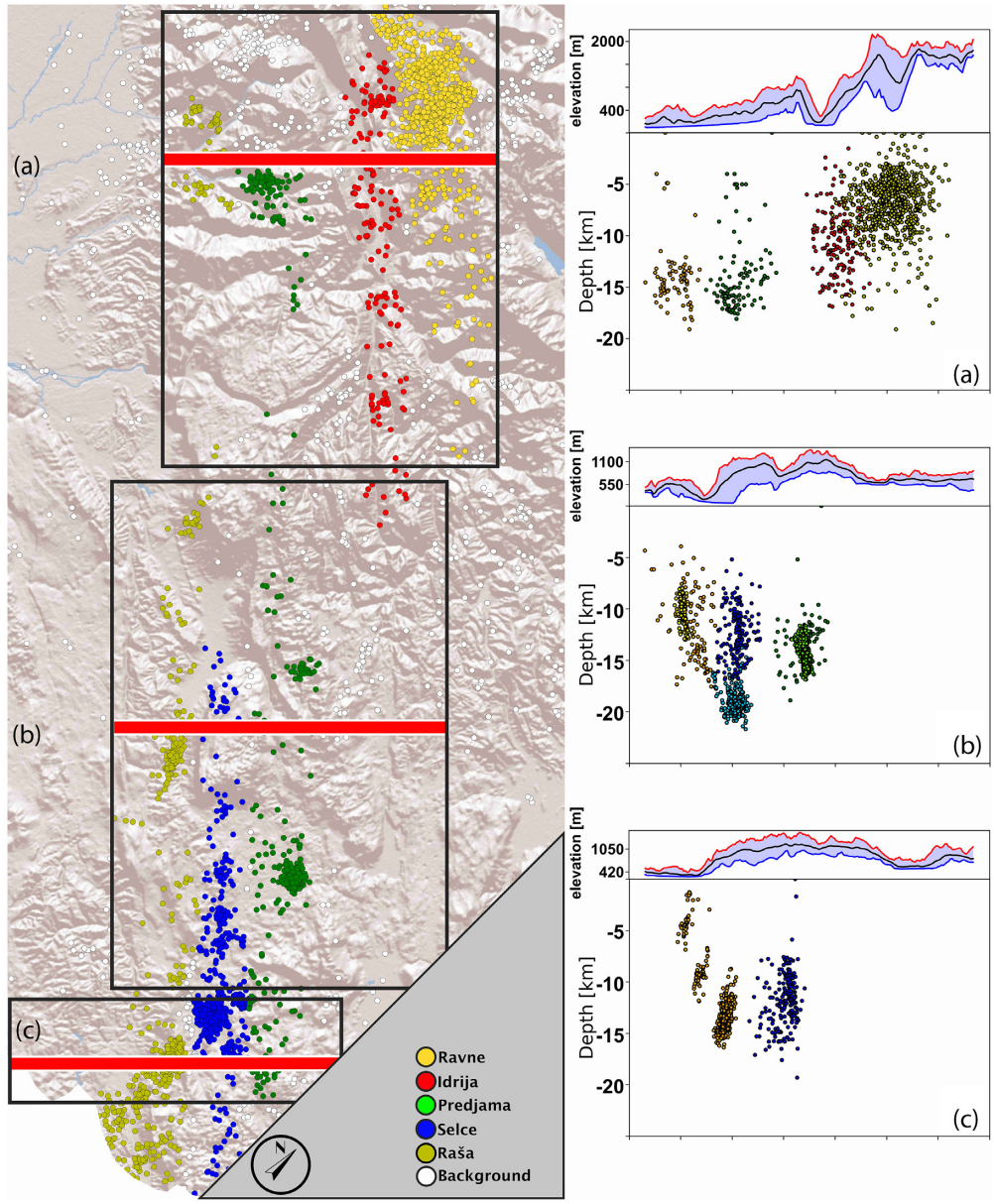

Figure 3. Map view and cross-sections perpendicular to the Idrija fault. Earthquakes are coloured regarding the causative fault. Detected and relocated earthquakes show that Idrija fault experiences earthquakes only along its northern segment, while the southern segment is locked. The transition between segments happens close to the town of Idrija, where Idrija fault exhibits a clear change from the geological (Mlakar *et al.* 2009) and geomorphologic (Moulin *et al.* 2016) point of view. Ravne fault NE from Idrija fault experienced the highest number of earthquakes in the studied time period but the seismicity is diffused, due to the complexity of the faulting in the area of transition from Southeastern Alps thrusting mechanisms to the strike-slip faulting of Northwestern External Dinarides. The cross section (a) shows earthquakes of Ravne, Idrija Predjama and Raša faults. Cross section (b) illuminates structure of vertical Predjama and Selce fault, and vertical at shallow depths and dipping at greater depths Raša fault. In the cross section (c) Raša fault is depicted from the clussters of relocated earthquakes which happened on the antithetic faults to Raša fault and vertical Selce fault. Above the cross sections elevation sketch profile is presented. In blue minumum elevation values are represented and in red maximum values. In black, along the profile values are ploted.

periods of elevated earthquake activity which show distinct migration in both time and space across the fault system (Fig. S3). The transient periods are dominated by different seismic swarms located at seismogenic depths. Transients are also reported at the surface as time-dependent deformation as seen on the extensometer located on the top of the Predjama fault inside the Postojna cave (Šebela *et al.* 2005; Gosar *et al.* 2009, 2011). This extensometer is the only one inside a cave in this region, therefore in a constant environmental conditions, with the highest sampling rate and the longest continuous time-series. The measurements started in May 2004 and exhibit both linear and transient behaviour within the surface deformation as shown on the angular deviation among the two horizonal and vertical components with a major contribution from the vertical one (Fig. 5). The seismic activity and the surface deformation vs time clearly highlight important transients across the Predjama fault as reported in Fig. 5. Specifically in the 2009–2010 period, the Postojna seismic swarm (Fig. 6, green circles) recorded at an average depth of 15 km on the Predjama fault coincides with a clear transient reported on the extensometer sitting on the top of the same fault. The surface deformation exhibits a gradient along the

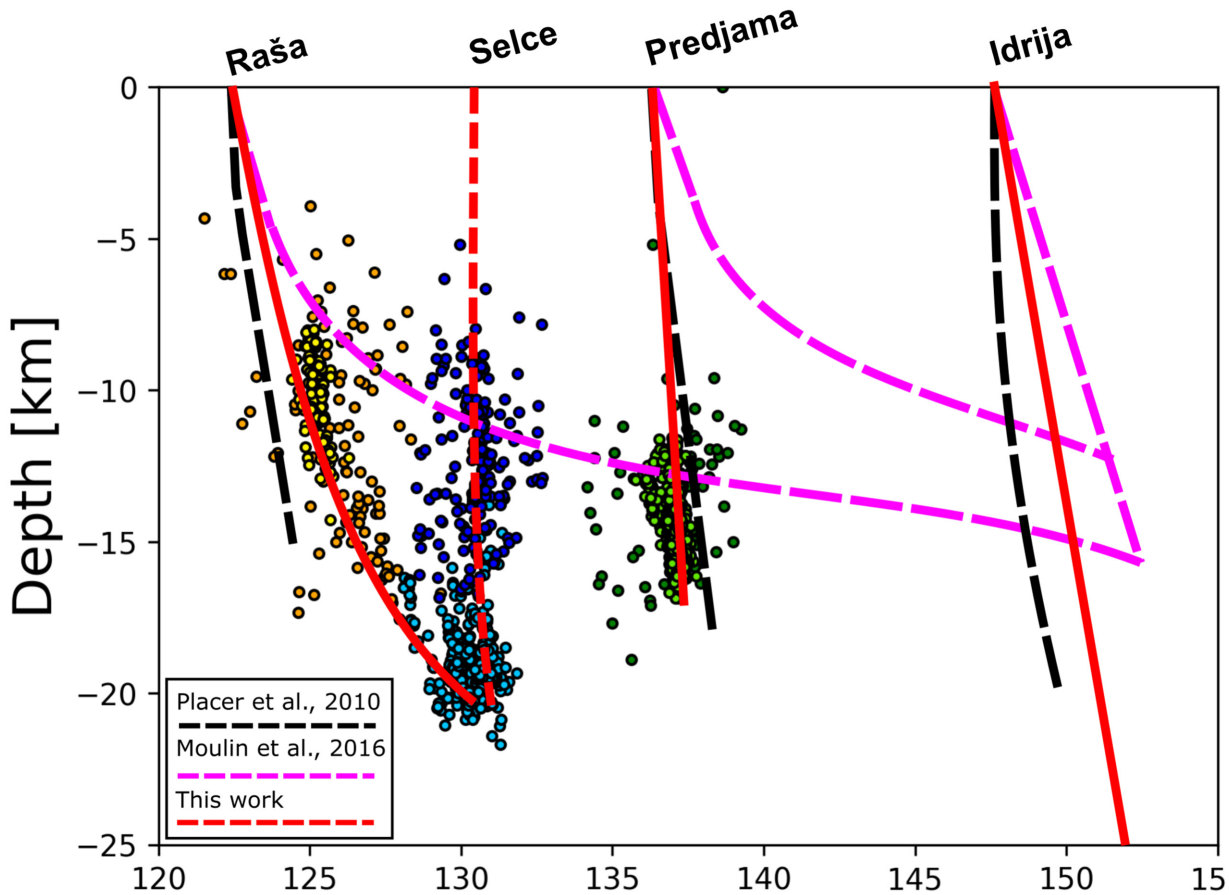

Figure 4. Newly constrained model of the central part of the fault system in western Slovenia. In red, our proposed model is shown as understood from geomorphology (Moulin *et al.* 2016), geodesy (Wang, private communication 2018) and seismology (Guidarelli *et al.* 2017). Idrija fault is locked in the central part and is not exhibiting any earthquakes while a clear vertical structure is observed for Predjama and Selce fault. Raša fault is a vertical structure in the shallow part and exhibits change in dip at depths. Red dotted line represents Selce fault, which is expressed on the surface. Selce fault is active as observed from relocated earthquakes but not treated as an active fault in previous studies (Atanackov *et al.* 2015).

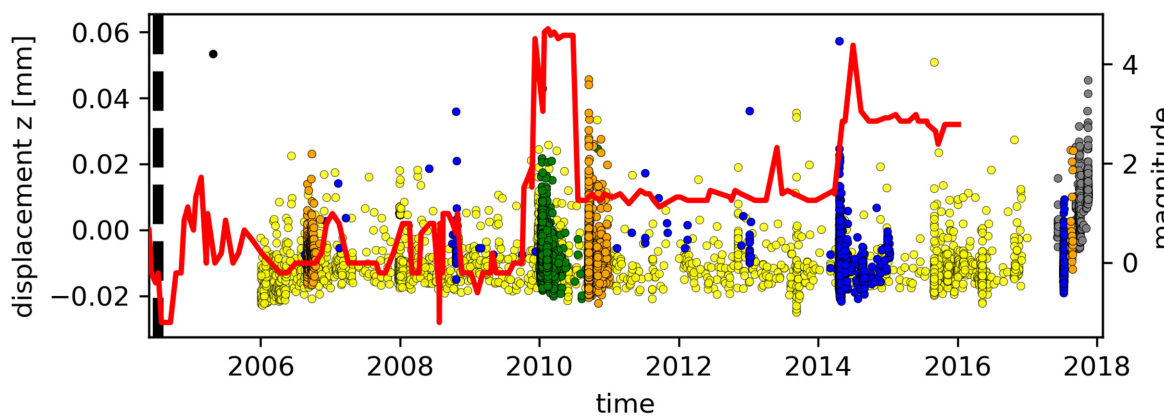

Figure 5. Extensometer data (red line) plotted with earthquakes detected along the Predjama fault (green), Selce fault (blue), Raša fault (orange), Ravne fault (yellow) and unknown fault in the south of the system (grey). Black dashed line represents timing of the 2004 M_W 5.2 earthquake, black dot is a local earthquake, south of Postojna extensometer. As seen on the extensometer data, two clear transient signals are observed coinciding with the local earthquake activity. The most prominent is the 2009–2010 transient coexisting with the elevated earthquake activity along Predjama fault and migration of earthquake sequences along Raša fault. The data shows vertical component of the extensometer, positive means subsidence of the NE block.

vertical axis (Gosar *et al.* 2011) with subsidence of the NE block reaching a plateau. This plateau which lasted for 4 months without major changes was followed by the signal suddenly dropping back to much lower value, reporting uplift of the NE block. The original position prior to the subsidence was not reached in the studied time interval. This transient in the extensometer deformation and earthquake activity started right after the initiation of a swarm-like sequence of similarly sized main shock–aftershock sequences (Fig. 6,

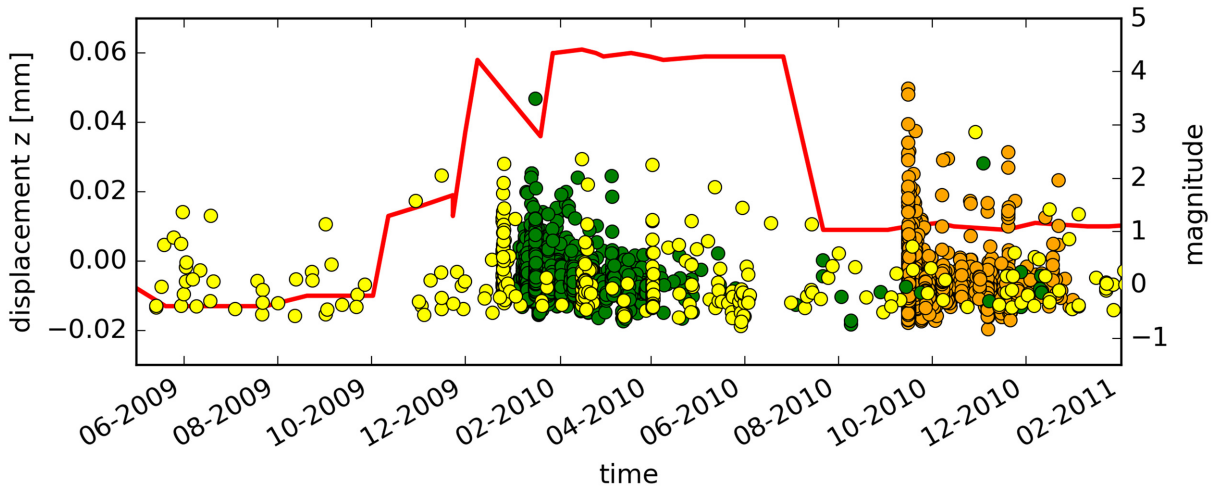

Figure 6. The 2009–2010 transient observed on the extensometer. Green dots are earthquakes of Postojna swarm, yellow Ravne fault sequences and orange Raša fault sequence.

yellow circles) that started to migrate along Ravne fault from north to south. In September 2010 a triple main shock–aftershock sequence (Fig. 6, orange circles) happened along the southern part of the Raša fault, where we could also observe a migration from north to south and from deeper to shallower depths, as already discussed in the previous section. This activity does not coincide with any deformation on the extensometer situated 25 km far away. The extensometer stayed at approximately the same level until an important gradient is reported in April 2014 (Fig. 5) coinciding with an earthquake distant 20 km away and with a M_w 4.5 on Selce fault. The extensometer stayed on a plateau up to 1 January 2016 when the data were not made available. Since then clustering in time and space of the earthquake activity happened again in the 2nd half of 2017 in the southernmost part of the faulting system, with small swarms and a main shock–aftershock sequence along Selce fault, small swarm along Raša fault and a longer lasting swarm and three stronger (magnitude above 4) earthquakes close to Rijeka in Croatia.

The earthquake distribution and extensometer data, over more than a decade of observations, report transients on the active fault system in western Slovenia except on the southern segment of the Idrija fault when compared to its northern segment. Idrija fault is now understood as the leading fault within the system. This is based on both its long-term behaviour as inferred from geomorphology (Moulin *et al.* 2016) and on its short-term behaviour as inferred from InSAR data (Wang, private communication, 2018) with similar slip rates of the order of 2 mm yr^{-1} on average. In the next section, we will analyse the effect of the interseismic loading along the southern segment of Idrija fault and the stress changes it generates on the adjacent regions where swarms and transients are reported.

Possible driving mechanism

Assuming a simple Coulomb friction model for earthquakes, change of Coulomb failure stress (King *et al.* 1994) will increase or decrease the potential for nucleation of an earthquake, as defined by:

$$\Delta CFS = \Delta\tau + \mu\,(\Delta\sigma_n + \Delta p)\,, \tag{1}$$

where $\Delta\tau$ is the shear stress change resolved in the preferred slip direction, $\Delta\sigma_n$ and Δp are the normal stress change (positive for unclamping on the fault) and pore pressure change on the fault, and μ is the coefficient of friction. It appears that ΔCFS as low as 0.1 bar can trigger the seismic activity (Rice & Cleary 1976; Reasenberg & Simpson 1992). Pore pressure can be related to normal stress using the following equation:

$$\Delta p = -\frac{\Delta\sigma_{kk}}{3}, \tag{2}$$

where B is the Skemption's coefficient and its value varies from 0 to 1 (Rice & Cleary 1976). Any sudden change in normal stress in a saturated porous medium causes a change in pore pressure. The pore pressure change will then tend to diminish by fluid diffusion at the rate determined by the local diffusivity of the system. Thus, fault clamping and unclamping, which strengthens and weakens the faults respectively, will change according to the changes in normal stresses or pore pressure changes. Fault unclamping will hence promote the earthquake activity along the fault and clamping will suppress it.

For the model estimation we used Coulomb 3.4 software (Toda *et al.* 2011). It uses analytical expressions provided by the Okada (1985, 1992) to estimate the Coulomb failure stresses (ΔCFS). Assuming homogeneous half-space elastic medium with shear modulus equal to 30 GPa, we computed ΔCFS for an average receiver fault geometry of the Idrija fault system with strike = 310°, dip = 80° and rake = 170° and present the results in the Supporting Information (Fig. S6). Here we present both shear and normal Coulomb stresses which were estimated from an interseismic loading on the southern segment of the Idrija fault at a locking depth of 18 km which is the average depth at which seismicity shuts-down in western Slovenia. ΔCFS was computed assuming $\mu = 0.4$ and $\mu = 0.8$. $\Delta CFS > 0.01$ bar yr^{-1} was estimated for an interseismic slip rate on Idrija fault set at 2 mm yr^{-1} (e.g. Moulin *et al.* 2016; Wang, private communication 2018). Assuming the constant creep rate, ΔCFS becomes greater than 0.1 bar after a decade. Figs 7–9 indicates that positive normal stress changes, reflecting unclamping, compares very well with the seismicity distribution. A constant loading from the Idrija fault at 0.01 bar yr^{-1} promotes earthquake activity by unclamping Predjama, Selce and Raša faults.

For temporal and spatial clustering of swarms, main shock–aftershock sequences, their migration (2009–2010 and 2017) and explanation of the extensometer measurements, additional short-time scale processes leading to pore pressure changes are to be

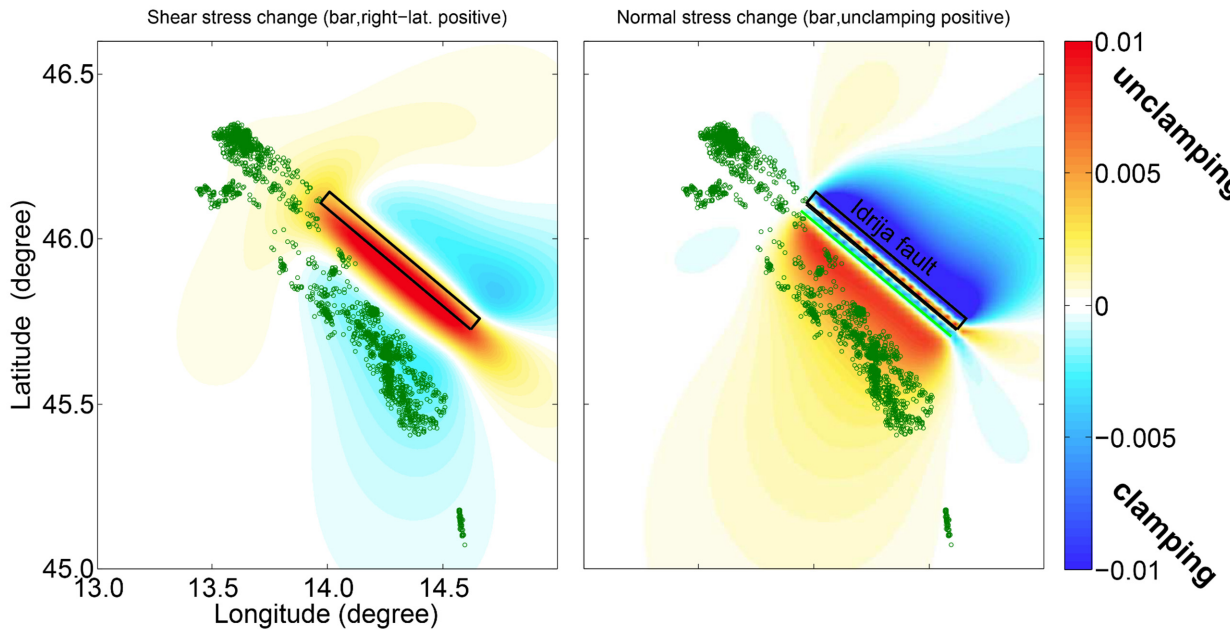

Figure 7. Shear (left-hand panel) and normal (right-hand panel) stress changes as computed for the locked southern segment of Idrija fault, creeping beneath 18 km. Green dots represent earthquakes along the faults parallel to Idrija fault. We can observe that normal stress changes (red—positive, blue—negative) can explain system wide earthquake activity by fault unclamping.

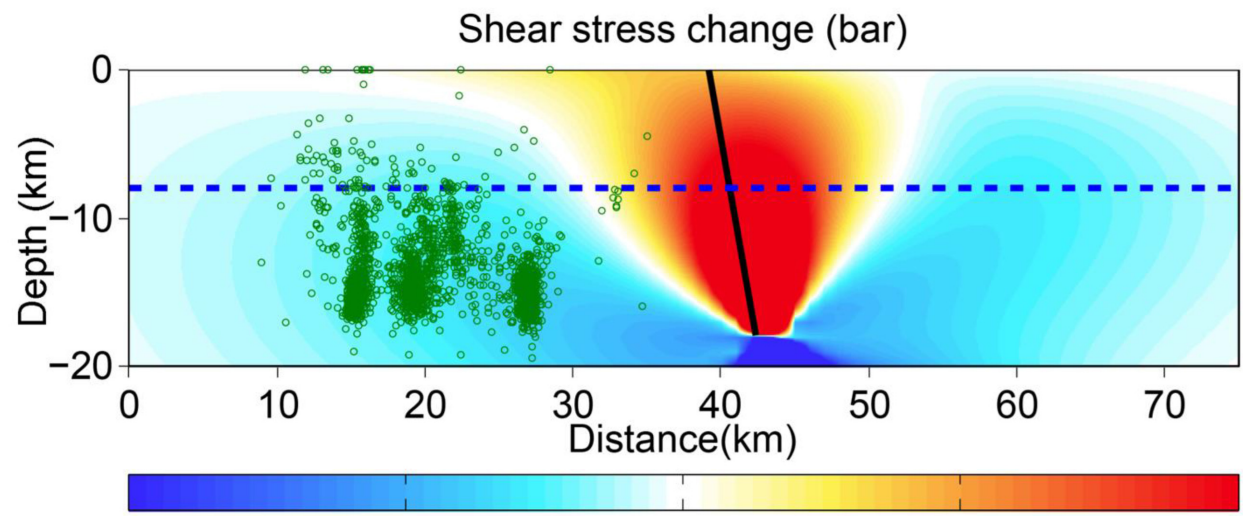

Figure 8. Same model as Fig. 7. A cross section perpendicular to the southern segment of Idrija fault for the shear stress changes model. Earthquake activity cannot be explained by shear stresses alone coming from Idrija fault.

considered. These processes may either be induced by fluid circulation and/or slow-slip as reported in other regions (*e.g.* Linde *et al.* 1996; Rousset *et al.* 2016).

The transient deformation that affected the Predjama fault in 2009 with a sudden increase of the surface deformation at the extensometer and a simultaneous swarm activity at seismogenic depths might likely be the velocity strengthening and weakening responses (Stuart 1988; Dieterich 1992) of a vertical and locked fault at its surface and depth terminations. This response can be driven by a slow-slip event on the deeper part of Idrija fault that would affect both the interseismic loading rate along with a change in the fluid circulation.

The downward motion, as seen on extensometer is a consequence of the increase in vertical stresses ($\sigma_v - \Delta p_h$) due to the extraction of fluids at depth in which $\sigma_v = pgh$ and Δp_h is the change in hydrostatic pressure. This would create a pressure gradient at the depth, increasing pore pressure in the regions where pore pressure decreased, coinciding with the earthquake swarm activity, beneath the Postojna block. With the end of transient slow-slip, pore pressures would diminish, and vertical stresses would decrease with time, reaching the equilibrium followed by the uplift of Predjama block. A diagram is shown in Fig. 10.

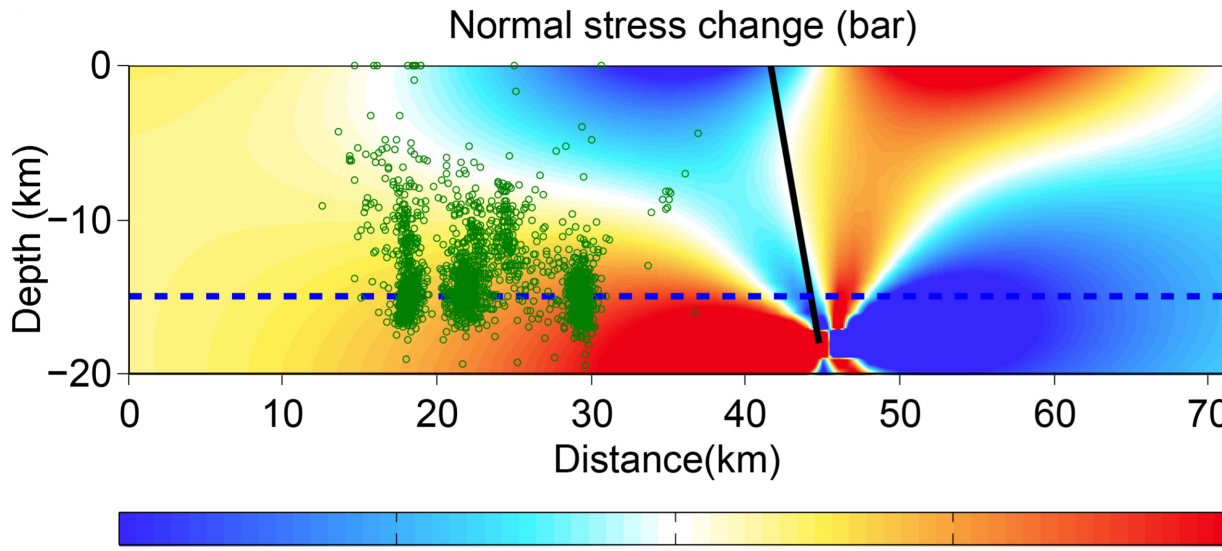

Figure 9. Same model as Fig. 7. A cross-section perpendicular to the southern segment of Idrija fault shows that normal stress changes can explain the earthquakes along all the faults parallel to Idrija fault on its western side, namely Predjama, Selce and Raša fault.

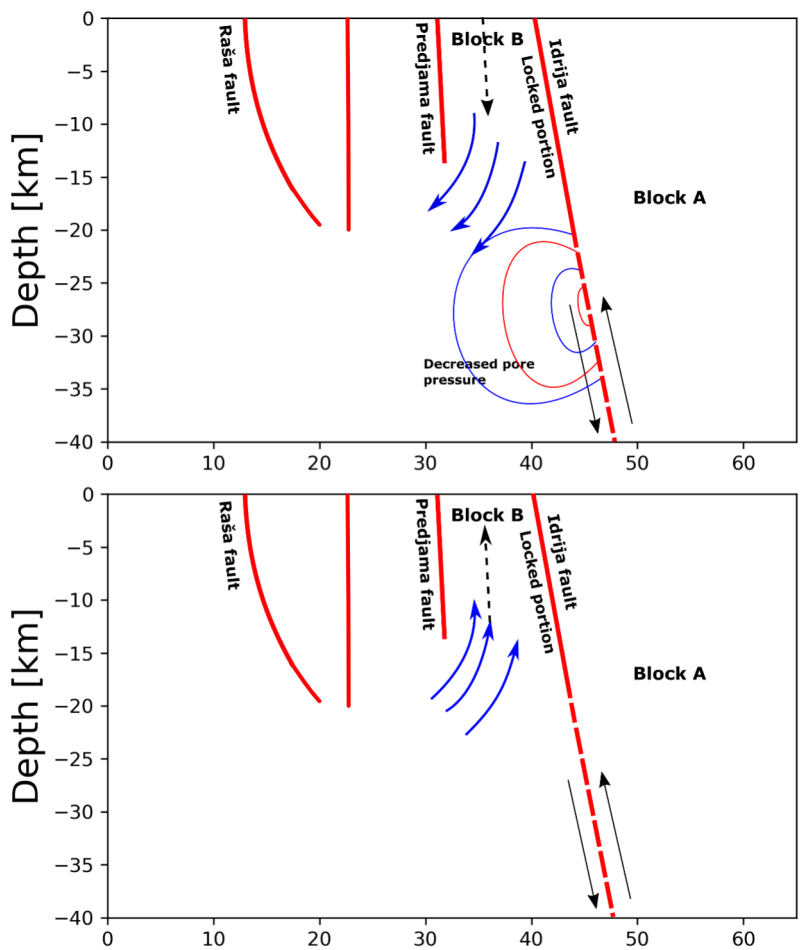

Figure 10. A diagram of possible fluid circulation (2009–2011) as a response to the slow-slip event along Idrija fault. A slow-slip event would effect normal stresses causing the migration of the fluids away from the Idrija fault (top panel) and subsidence of the Block B. After the slow-slip event (bottom panel), negative pore pressures (relative to the elevated pore pressures west of Predjama fault) would cause the return of fluids and uplift of the Block B.

DISCUSSION AND CONCLUSIONS

The newly detected and relocated earthquakes in western Slovenia between 2006 and 2017 illuminate the geometry of five nearly parallel faults namely: Ravne fault, Idrija fault, Predjama fault, Selce fault and Raša fault. All these faults do have an expression in the geomorphology. Raša fault, being the external and southwestern-most fault of the system exhibits a change in geometry from nearly vertical at the surface to high dip angle at a depth larger than 10 km. Selce fault is a vertical fault reaching a depth of at least 20 km as exhibited by the relocated earthquakes. This fault probably connects at depth with Raša fault. Geometry of Predjama fault is complex along strike but with a linear vertical downdip extent down to 20 km. The leading fault in the system is Idrija fault which experiences earthquake activity from 5 to 20 km on its northern segment while on its southern segment no earthquake activity was detected.

The clustering in time and space of the relocated earthquakes is most likely in favour of an unclamping mechanism induced either by a cumulative interseismic loading on the southern segment of Idrija or by individual slow-slip events that may corroborate the different seismic swarms taking place at seismogenic depths close to the velocity strengthening transition. Further to these processes, fluid circulations and pore pressure changes may be required to explain singular transients as the one observed on the Predjama fault. Specifically, in 2009 the Predjama fault accommodated a sudden increase of the surface deformation at the extensometer accompanied by a simultaneous swarm activity at its seismogenic depth. This behaviour might correspond to velocity strengthening and weakening processes taking place at both the surface and depth terminations of a locked vertical fault. These processes can be driven by a slow-slip event on the deeper part of Idrija fault that would generate a temporary acceleration of the interseismic loading rate and a change within fluid circulation.

Our newly constrained geometry of the active fault system in western Slovenia is of paramount importance in earthquake hazard evaluation. The vertical and along strike extent of the active faults can favour earthquakes of moment magnitude equal to 7 or larger. The most recent large earthquake that occurred in this region is the 1511 earthquake with a magnitude 6.8.

ACKNOWLEDGEMENTS

Blaž Vičič thanks for the support from 'fondi del Commissariato del Governo nella Regione Friuli Venezia Giulia ('Fondo Trieste')' through the University of Trieste. We thank the Karst Research Institute from Slovenia for the extensometer data which they provided. The extensometer monitoring was accomplished within EPOS IP H2020 project with ZRC SAZU, Slovenia as partner. This work is done in the framework of the ICTP-Generali Earthquake Hazard Programme. We would like to thank Alessandro Vuan and anonymous reviewers for their comments.

REFERENCES

Aoudia, A., Saraò, A., Bukchin, B. & Suhadolc, P., 2000. The 1976 Friuli (NE Italy) thrust faulting earthquake: a reappraisal 23 years later, *Geophys. Res. Lett.,* **27**(4), 573–576.

Atanackov, J., Jamšek Rupnik, P., Celarc, B., Jež, J., Novak, M. & Milanič, B., 2015. *Seizmotektonska Parametrizacija Aktivnih Prelomov Slovenije*, Geološki zavod Slovenije.

Bajc, J., Aoudia, A., Sarao, A. & Suhadolc, P., 2001. The 1998 Bovec-Krn Mountain (Slovenia) earthquake sequence, *Geophys. Res. Lett.,* **28**(9), 1839–1842.

Basili, R., Valensise, G., Vannoli, P., Burrato, P., Fracassi, U., Mariano, S., Tiberti, M.M. & Boschi, E., 2008. The Database of Individual Seismogenic Sources (DISS), version 3: summarizing 20 years of research on Italy's earthquake geology, *Tectonophysics,* **453**(1-4), 20–43.

Bavec, M. *et al.*, 2013. Evidence of Idrija fault seismogenic activity during the Late Holocene including the 1511 Mm 6.8 earthquake, in *Proceedings of the 4th International INQUA Meeting on Paleoseismology, Active Tectonics and Archeoseismology,* pp. 23–26, Grützner & Reicherter Geosolutions Aachen.

Borghi, A., Aoudia, A., Riva, R.E. & Barzaghi, R., 2009. GPS monitoring and earthquake prediction: a success story towards a useful integration, *Tectonophysics,* **465**(1-4), 177–189.

BRTT Antelope software, 1995. http://brtt.com/software.html.

Chamberlain, C.J., Boese, C.M. & Townend, J., 2017. Cross-correlation-based detection and characterisation of microseismicity adjacent to the locked, late-interseismic Alpine Fault, South Westland, New Zealand, *Earth planet. Sci. Lett.,* **457,** 63–72.

Di Bona, M., 2016. A local magnitude scale for crustal earthquakes in Italy, *Bull. seism. Soc. Am.,* **106**(1), 242–258.

Dieterich, J.H., 1992. Earthquake nucleation on faults with rate-and state-dependent strength, *Tectonophysics,* **211**(1-4), 115–134.

Fitzko, F., Suhadolc, P., Aoudia, A. & Panza, G.F., 2005. Constraints on the location and mechanism of the 1511 Western-Slovenia earthquake from active tectonics and modeling of macroseismic data, *Tectonophysics,* **404**(1-2), 77–90.

Gosar, A., Šebela, S., Koštak, B. & Stemberk, J., 2009. Surface versus underground measurements of active tectonic displacements with TM 71 exstensometers in Slovenia, *Acta Carsol.,* **38**(2-3).

Gosar, A., Šebela, S., Košťák, B. & Stemberk, J., 2011. On the state of the TM 71 extensometer monitoring in Slovenia: seven years of micro-tectonic displacement measurements, *Acta Geodyn. Geomater.,* **8**(4), 389–402.

Guidarelli, M., Aoudia, A. & Costa, G., 2017. 3-D structure of the crust and uppermost mantle at the junction between the Southeastern Alps and External Dinarides from ambient noise tomography, *Geophys. J. Int.,* **211**(3), 1509–1523.

Jesenko, T., Cecić, I., Čarman, M., Stopar, M.L. & Živčić, M., 2006. Earthquakes in Slovenia in 2006. http://www.arso.gov.si/potresi.

Jesenko, T., Cecić, I. & Živčić, M., 2010. M. Čarman, 2011: Potresi v Sloveniji leta 2010, 17–35. http://www.arso.gov.si/potresi.

Kastelic, V., Živčić, M., Pahor, J. & Gosar, A., 2006. Seismotectonic characteristics of the 2004 earthquake in Krn mountains, *Potresi v letu 2004,* Slovenian Environment Agency, 78–87. http://www.arso.gov.si/potresi.

Kennet, B.L.N., 1991. IASPEI 1991 seismological tables, *Terra Nova,* **3**(2), 122–122.

King, G.C., Stein, R.S. & Lin, J., 1994. Static stress changes and the triggering of earthquakes, *Bull. seism. Soc. Am.,* **84**(3), 935–953.

Linde, A.T., Gladwin, M.T., Johnston, M.J., Gwyther, R.L. & Bilham, R.G., 1996. A slow earthquake sequence on the San Andreas fault, *Nature,* **383**(6595), 65.

Lohman, R.B. & McGuire, J.J., 2007. Earthquake swarms driven by aseismic creep in the Salton Trough, California, *J. geophys. Res.: Solid Earth,* **112**(B4).

Lomax, A., 2004. Probabilistic, non-linear, global-search earthquake location in 3D media, Anthony Lomax Scientific Software, Mouans–Sartoux, France.

Metois, M. *et al.*, 2015. Insights on continental collisional processes from GPS data: dynamics of the peri-Adriatic belts, *J. geophys. Res.: Solid Earth,* **120**(12), 8701–8719.

Mlakar, I., Čar, J., Placer, L. & Ogorelec, B., 2009. *Geološka Karta Idrijsko-Cerkljanskega Hribovja Med Stopnikom in Rovtami 1: 25.000: Geological map of the Idrija-Cerkno hills between Stopnik and Rovte 1: 25.000,* Geološki zavod Slovenije.

Moulin, A., Benedetti, L., Gosar, A., Rupnik, P.J., Rizza, M., Bourlès, D. & Ritz, J.F., 2014. Determining the present-day kinematics of the Idrija fault (Slovenia) from airborne LiDAR topography, *Tectonophysics,* **628,** 188–205.

Moulin, A. *et al.*, 2016. The Dinaric fault system: Large-scale structure, rates of slip, and Plio-Pleistocene evolution of the transpressive northeastern boundary of the Adria microplate, *Tectonics,* **35**(10), 2258–2292.

Okada, Y., 1985. Surface deformation due to shear and tensile faults in a half-space, *Bulletin of the seismological society of America,* **75.4**(8):1135–1154.

Okada, Y., 1992. Internal deformation due to shear and tensile faults in a half-space, *Bulletin of the seismological society of America,* **82.2**(8):1018–1040.

Placer, L., Vrabec, M. & Celarc, B., 2010. The bases for understanding of the NW Dinarides and Istria Peninsula tectonics, *Geologija,* **53**(1), 55–86.

Reasenberg, P.A. & Simpson, R.W., 1992. Response of regional seismicity to the static stress change produced by the Loma Prieta earthquake, *Science,* **255**(5052), 1687–1690.

Ribarič, V., 1982. *Seismicity of Slovenia; Catalogue of Earthquakes (792 AD–1981),* Seizmološki zavod SR Slovenije.

Rice, J.R. & Cleary, M.P., 1976. Some basic stress diffusion solutions for fluid-saturated elastic porous media with compressible constituents, *Rev. Geophys.,* **14**(2), 227–241.

Rousset, B., Jolivet, R., Simons, M., Lasserre, C., Riel, B., Milillo, P., Çakir, Z. & Renard, F., 2016. An aseismic slip transient on the North Anatolian Fault, *Geophys. Res. Lett.,* **43**(7), 3254–3262.

Rutledge, Jim T., Phillips, William S. & .Mayerhofer, M. J, 2004. Faulting induced by forced fluid injection and fluid flow forced by faulting: An interpretaition of hydraulic-fracture microseismicity, Carthage Cotton Valley gas field, Texas, *Bulletin of the Seismological Society of America,* **94.5,** 1817–1830.

Saraò, A., 2016. On line catalogue of moment tensor solutions of earthquakes occured in NE Italy and its surroundings since 2014–2016. http://rts.crs.inogs.it.

Saraò, A. & Staff, C.R.S., 2013. On line catalogue of moment tensor solutions of earthquakes occured in NE Italy and its surroundings since 2009. http://rts.crs.inogs.it.

Shelly, D.R., Beroza, G.C. & Ide, S., 2007. Non-volcanic tremor and low-frequency earthquake swarms, *Nature,* **446**(7133), 305.

Stuart, W.D., 1988. Forecast model for great earthquakes at the Nankai trough subduction zone, *Pure appl. Geophys.,* **126**(2-4), 619–641.

Stucchi, M. *et al.*, 2013. The SHARE European earthquake catalogue (SHEEC) 1000–1899, *J. Seismol.,* **17**(2), 523–544.

Toda, S., Stein, R.S., Sevilgen, V. & Lin, J., 2011. Coulomb 3.3 graphic-rich deformation and stress-change software for earthquake, tectonic, and volcano research and teaching-user guide (No. 2011-1060), US Geological Survey.

Vrabec, M. & Fodor, L., 2006. Late Cenozoic tectonics of Slovenia: structural styles at the Northeastern corner of the Adriatic microplate, in *The Adria Microplate: GPS Geodesy, Tectonics and Hazards,* pp. 151–168, Springer.

Waldhauser, F., 2001. hypoDD—a program to compute double-difference hypocenter locations (hypoDD version 1.0-03/2001), *US Geol. Surv. Open File Rep., 01,* **113**.

Weber, J., Vrabec, M., Pavlovčič-Prešeren, P., Dixon, T., Jiang, Y. & Stopar, B., 2010. GPS-derived motion of the Adriatic microplate from Istria Peninsula and Po Plain sites, and geodynamic implications, *Tectonophysics,* **483**(3-4), 214–222.

Yoshida, K., Hasegawa, A., Yoshida, T. & Matsuzawa, T., 2018. Heterogeneities in stress and strength in tohoku and its relationship with earthquake sequences triggered by the 2011 M9 Tohoku-Oki earthquake, *Pure appl. Geophys.,* 1–21.

Zupančič, P., Cecić, I., Gosar, A., Placer, L., Poljak, M. & Živčić, M., 2001. The earthquake of 12 April 1998 in the Krn Mountains (Upper Soča valley, Slovenia) and its seismotectonic characteristics, *Geologija,* **44**(1), 169–192.

Šebela, S., 2016. Tectonic sights of the Pivka basin, *Acta Carsol.,* **34**(3), .

Šebela, S., Gosar, A., Košťák, B. & Stemberk, J., 2005. Active tectonic structures in the W part of Slovenia–Setting of micro-deformation monitoring net, *Acta Geodyn. Geomater,* **2**(1), 45–57.

SUPPORTING INFORMATION

Supplementary data are available at *GJI* online.

Figure S1. In the map of the region of interest, station used for matched-filter detection of earthquakes are represented in red, while the station used only in STA/LTA and manual inspection of waveforms are shown in cyan. Red lines represent the active faults of western Slovenia and red dots the locations of the templates used for matched-filter detection of earthquakes.

Figure S2. Magnitude of completeness of the two catalogues. The magnitude of completeness of ISC catalogue is 0.9. The magnitude of completeness for final catalogue was lowered to -0.1 mainly due to the addition of low magnitude swarm events and missed earthquake activity along Ravne fault.

Figure S3. Top figure shows earthquake activity through time perpendicular to the system of active faults in western Slovenia, coloured according to the active fault. The histogram represent total number of earthquakes per month of selected fault. Bottom figure is the same as top, but only for the time from 2009 to 2011 when the investigated migration of swarms and main shocks happened.

Figure S4. Comparison between 1-D IASP91 velocity model (black) used for initial locations and 3-D model used for relocation of earthquakes. 3-D model is slightly faster in the shallow part, resulting in slightly deeper locations of relocated earthquakes. Different colours of the 3-D velocity model represent different subareas of the original regional model.

Figure S5. Left figure represents horizontal errors of earthquakes located using IASP91 (green) model and 3-D velocity model (blue). As observed in the figure, the horizontal errors do not change drastically. Right figure shows vertical errors using IASP91 model (green) and 3-D model (blue). We observe lowering of the errors after relocation.

Figure S6. ΔCFS as computed using the same parameters as for normal and shear stresses. We used $\mu = 0.4$ for the left figure and $\mu = 0.8$ for right figure. We can observe that change in normal stresses and unclamping of the faults better explains earthquake activity along the active fault of western Slovenia.

Figure S7. Magnitude of completeness for the individual swarms observed along the active faults of western Slovenia. (a) Vipava swarm 2006, (b) Postojna swarm 2010, (c) Selce swarm 2017, (d) Ilirska Bistrica swarm 2017 and (e) Rijeka swarm 2017.

Figure S8. Locations and timings of the swarms discussed in the Swarms section of the paper. As mentioned in the paper, swarms are present only in the central and southern part of the fault system along all the faults.

Table S1. Locations and origin times of templates used for matched-filter detection of earthquakes.